Experimental Stark Profile Determination of Some Plasma Broadened He I- and He II-Lines

H. Soltwisch * and H. J. Kusch

Institut für Experimentalphysik der Universität Kiel

Z. Naturforsch. **34a**, 300–309 (1979); received November 23, 1978

Line profiles of the plasma broadened lines He I: 3188, 3889, and 5016 Å and He II: 3203, 4686 Å have been determined from measurements using a wall-stabilized quasistationary pulsed discharge as a plasma source of sufficient homogeneity. The profiles were recorded applying the rapid-scan technique to enable single-shot registration of the spectral data. Electron density values were obtained from plasma-refractivity measurements at two different wavelengths using rare gas ion-lasers as background light-sources. The electron density range in this experiment was $(0.7-1.2) \cdot 10^{17}$ cm^{-3}. Temperature values of pure helium plasmas resulted from absolute radiation measurements (line intensities of He II 3203 Å and 4686 Å), yielding $\sim 4 \cdot 10^4$ K. In helium-hydrogen mixtures further used for plasma generation in the lower temperature region, temperature values could be estimated from the optically thick Balmer line H_α, yielding $\sim 2 \cdot 10^4$ K.

Experimental line shapes and half-widths are compared with the theoretical predictions of several authors and with the results of previous measurements. In case of neutral helium lines experimental and theoretical values agree within experimental accuracy (10%), whereas for the He II-lines the measured line shapes deviate considerably from the theoretical predictions.

A. Introduction

Stark broadening of spectral lines caused by electric field interaction with electrons and ions in plasmas has been subject to a great number of theoretical and experimental investigations. Since Stark broadened line shapes depend mostly on the density of charged particles in a plasma, theoretical line profiles of this type offer a convenient chance to determine electron density values in a plasma even when the temperature is known only approximately.

Hydrogen line profiles — especially for the Balmer line H_β — play here an outstanding role; line shape calculations of this line have proved to be reliable within at least 5% in the electron density range $(0.1-1.5) \cdot 10^{17}$ cm^{-3} (for theoretical and experimental results see Griem [1], [24]). Unfortunately in high electron density plasmas the H_β-line becomes rather broad (full half-width ~ 50Å at $N_e = 10^{17}$ cm^{-3}), causing a need for narrower lines — like He I- and He II-lines — for electron density determination.

B. A Review of Preceding Investigations

Stark broadened line profiles of isolated helium lines have been calculated by Griem, Baranger, Kolb and Oertel [2] (GBKO), and the results of these calculations have been tested in a large number of experimental studies [3–10]; further experimental study is of great advantage. GBKO-approximations are confirmed within $\pm 20\%$ by experimental investigations, however, some authors determined deviations between experimental and theoretical half-widths by a factor of 1.7 ([7, 8]). Stark broadening of the hydrogen-like He II-lines can be calculated according to theoretical procedures of Griem and Shen [11], Kepple [12], and Greene [13]. Several experimental studies ([3], [8], [14]–[19]) indicate, that the half-widths of the lines He II 3203 Å and 4686 Å are predicted well by the Griem-Shen approaches. The more recent calculations of Kepple [12] yield too broad profiles, whereas calculations of Greene [13] for the 4686 Å-line result into profiles with substantially enhanced peak intensities and reduced half-widths. All experiments concerning lines of ionized helium were performed in pulsed discharges, and in most of these investigations line profiles were scanned by the use of shot-to-shot techniques requiring high reproducibility of the applied light-sources.

By the use of an optical multichannel analyzer Bacon et al. [18] determined complete line profiles in a single-shot procedure.

---

* Present address: Institut für Plasmaphysik der KFA Jülich, D-5170 Jülich.

Reprint requests to Dr. H. J. Kusch, Institut für Experimentalphysik der Universität Kiel, Olshausenstr. 40/60, D-2300 Kiel.

0340-4811 / 79 / 0300-0300 $ 01.00/0

C. A Survey of the Present Investigation

In this work we performed experimental studies on three lines of neutral helium (λ 3188, 3889 and 5016 Å) and on two Fowler series lines (λ 3203 and 4686 Å).

The plasma under investigation was produced in quasistationary wall-stabilized discharges, and the line profiles were recorded by the use of a rapid-scan technique applying a monochromator with a rotating grating, thus avoiding the disadvantages of repeated-shot measurements. Electron density values of high accuracy were determined from plasma-refractivity measurements applying an interferometer of the Michelson type operated at two different wavelengths (see [20]). A special goal of the present work were improved Stark broadening parameters, especially for the lines in the He II-system. As mentioned above, earlier measurements sufferred severely from inaccurate spectral-intensity recording due to the lack of reproducibility of the plasma parameters. Consequently only few comparisons have been made yielding complete line profiles ([14], [15], [16], [18]).

In order to clear up the discrepancies to the GBKO-approach (see [24]) seen in some experiments [7], [8], plasma radiation was measured by the use of improved procedures.

D. The Experimental Device

a) The Plasma Source

1. The Discharge Tube

As a light-source for our investigations we used a wall-stabilized pulsed discharge as earlier described by Kusch and Mewes [21], which had been applied to numerous studies of line broadening research up to now. A cylindrical glass tube of 27 mm inner diameter and 120 mm length was used as discharge vessel, and two copper-discs were fitted onto the ends of the tube feeding the discharge current to the plasma column, and being sealed vacuum-tight by means of outer O-rings. To permit end-on-observation of the plasma column, the electrodes had a central bore, into which small Al_2O_3-tubes (DEGUSSIT AL 23) with quartz windows were inserted varying the length of the plasma column (in the line of sight). Figure 1 shows a cross-sectional view of the cathode-unit (the anode-unit was constructed similarly).

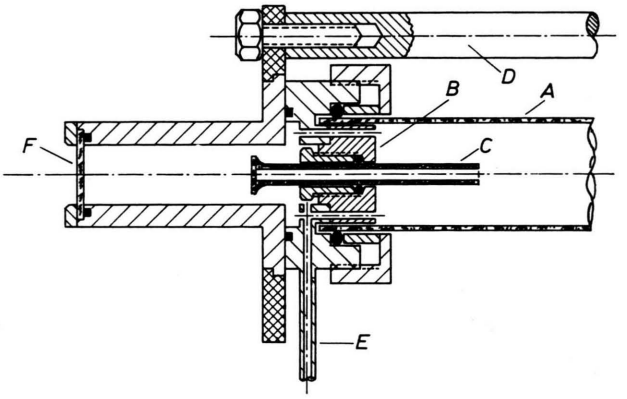

Fig. 1. Sectional view of the discharge tube cathode unit. A: discharge tube sealed by O-rings; B: copper electrode; C: Al_2O_3-tube with quartz windows; D: one of the three plastic rods connecting the total discharge tube; E: to vacuum- and filling-system; F: quartz window.

The discharge tube was filled up to the desired pressure with pure helium (purity 99.99%) or with a helium-hydrogen mixture (50:50%); filling pressures of 5—15 torr were used.

Magnetically caused distortions of the plasma column were reduced by leading the current through three back-straps arranged symmetrically around the discharge tube.

2. The Power Supply

Rectangular pulses of 180 μsec duration with a maximum current of 10 kA were supplied from a LC-network (10 capacitors 20 μF/10 kV each, connected with coils of 4 μH each) with a terminating resistance of 0.45 Ω, equal to the characteristic impedance of the circuit. Overswinging in the initial phase of the pulse could be reduced by enlarging the output inductance to 6 μH. The capacitor bank was discharged via a spherical spark gap which could be triggered by external signals.

b) Plasma Homogeneity Checks

The homogeneity of the plasma column along the axis of the discharge tube was checked in a series of preparatory investigations. By the use of a framing camera and two different interference filters in front of the camera lens short-time pictures of the discharge were taken exposed for 1 μsec. The filters had a passband of ~ 50 Å centered at the He II-line 4686 Å (a line of high sensitivity for changes in temperature) or at the line He I 5016 Å. Simultaneously end-on intensities of the helium lines were monitored applying a monochromator of 0.5 m focal

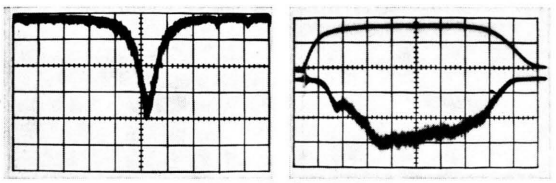

a b

Fig. 2a. Scope trace of a He II 4686 Å line profile resolved by rapid-scan techniques. Sweep rate: 5 μsec/div. corresponding to 5.03 Å/div.

Fig. 2b. Discharge current (upper trace) and peak intensity of the line He II 4686 Å (lower trace) vs. time. Sweep rate: 20 μsec/div.

length. Except for pictures exposed during the rising phase of the current pulse or at filling pressures >15 torr all photographs showed slightly bent but uniformly bright plasma columns. Stratified structures, dark spots or filaments indicating regions of lower temperature were not observed. In a second experiment radial distributions of the line emission coefficients of He I 5016 Å and He II 4686 Å were determined. Each of the cross-sections under observation was focussed side-on onto a 128 element photodiode-array (RETICON) equipped in front with interference filters. Ignoring continuous radiation distributions and the influence of curved discharge tube walls [22], radial profiles of emissivity were derived by Abel's inversion [23] of the diode signals. Emission coefficients were found nearly constant in a cylinder of up to 10 mm diameter around the tube axis. Finally checks have been performed to study the constancy of electron density along the line of sight (the discharge axis). Protruding the Al_2O_3-tubes appropriately into the plasma, eight sections of the plasma column of equal length could be selected, and the line integrals were determined by the interferometric technique to be described in Chapt. E, b). Apart from slight deviations due to the non-reproducibility of the light-source no systematic influence of the plasma-path position between the electrodes was found.

According to the Griem estimates [24] relaxation times for the establishment of excitation and ionization equilibrium conditions were small compared with the duration of quasistationary plasma states ($\leqq 1$ μsec for a helium plasma with $N_e \sim 10^{17}$ cm^{-3} and $kT \sim 4$ eV).

On the other hand demixing of the plasma constituents caused by diffusion effects in He-H-plasmas become important only after some m sec pulse duration [7] and thus need not be considered here.

E. Plasma Data Registration

a) Line Profile Registration Techniques

Line profiles were recorded in a rapid-scan technique by means of an Ebert monochromator equipped with a quickly rotating grating thus yielding spectral line profiles during the quasistationary state of the plasma. Constructional data of the instrument were: focal length 100 cm, rotation frequency of the grating: $\omega = 2\pi \cdot 10$ sec^{-1}, ruled area of the grating 50×50 mm^2 with 1200 grooves/mm ($= 1/g$). From these data a reciprocal dispersion of 8.3 Å/mm in the focal plane, a theoretical resolution of $6 \cdot 10^4$ and, at least, a spectral registration speed of ~ 1 Å/μsec in the first order is obtained, applying the well-known grating formula which results in:

$$d\lambda/dt = \omega(4g^2 - \lambda^2)^{1/2}; \quad (1)$$

experimental values of $d\lambda/dt$ were obtained by displaying the spectrum of a low-pressure mercury discharge together with a sequence of time-marks on a double-beam oscilloscope.

Photoelectric recording of the spectra was achieved throughout using photomultiplier tubes — RCA 1 P 28 for the spectral range $3000 \leqq \lambda \leqq 5100$ Å, while for the registration of the Balmer line H_α RCA type 4832 was applied. For time-correlation between the position of the rotation grating (of the monochromator) and the recording set up a small auxiliary mirror was fixed to the rotation axis reflecting the beam of a helium-neon laser onto an adjustable photo-diode thus producing a number of subsequent pulses at predetermined grating positions for trigger uses. Electronic gates selected only one initial pulse for a quartz-stabilized delay circuit with six independent units controlling the timing of the total experimental procedure.

The instrumental profile of the spectrometer was determined using the 4880 Å-line of an argon-ion laser and was found to be close to a Gaussian profile with a (full) half-width of 0.46 Å.

b) Electron Density Determination by Interferometric Techniques

1. The Theoretical Background

Electron density values were derived from two-wavelengths interferometry measurements. Due to the large dispersion of the electronic component of the plasma compared with the influence of other constituents simultaneous measurements of plasma

refractivity offer a most convenient method for the direct determination of the electron density, even when non-electronic particles in the plasma contribute considerably to the total refractivity. In detail the refractivity of a (dilute) plasma is given by:

$$n(\lambda) - 1 = 2\pi \sum_{a,i,k} \alpha_a^{i,k}(\lambda)\, N_a^{i,k} - \frac{e^2 \lambda^2}{2\pi m_e c^2} N_e \qquad (2)$$

(see [20]), wherein $N_a^{i,k}$ denotes the number density of a species a in the i^{th} ionized and k^{th} excited state; $\alpha_a^{i,k}$ is the (respective) polarizability; e, m_e and c are here the universal constants. Experimental polarizabilities are available for most neutral species ground states, and their dependence on wavelength far away from resonance-lines is well-represented by the one-term Cauchy formula:

$$\alpha_a = A_a + B_a/\lambda^2; \qquad (3)$$

the index: a stands' for "atomic".

Using numerical values for A_a and B_a based on the data pulished by Allen [25] and concerning the wavelengths $\lambda_1 = 5145$ Å and $\lambda_2 = 6471$ Å for (neutral) helium is found:

$$\frac{\alpha_{He}(6471\text{ Å})}{\alpha_{He}(5145\text{ Å})} = \frac{\lambda_1^2(A_{He}\lambda_2^2 + B_{He})}{\lambda_2^2(A_{He}\lambda_1^2 + B_{He})} = 0.997. \qquad (4)$$

Polarizabilities of excited states or for ionized particles are only approximately known, but they can also be assumed to be only weak functions of wavelength, especially at probing wavelengths sufficiently far remote from plasma emission lines.

Under the conditions of the experiment noticeable influence might be expected only from H_α (6563 Å) near to the krypton-laser wavelength; but following Griem [24], refractivity changes caused by hydrogen atoms in the second excited state are estimated to be more than two orders of magnitude lower than the refractivity caused by the electron component only.

Number density values of either ionized or excited particles are substancially lower than ground state contributions, and approximating all non-electronic plasma constituents with the same wavelength dependence of refractivity, Eq. (2) yields:

$$0.997[n(\lambda_1) - 1] - [n(\lambda_2) - 1] = -\frac{e^2}{2\pi m_e c^2}(0.997\,\lambda_1^2 - \lambda_2^2) N_e. \qquad (5)$$

2. The Experimental Set Up

Simultaneous determination of plasma refractivity values $n(\lambda) - 1$ at two different wavelengths was performed by means of an interferometer of the Michelson type, applying two noble-gas ion lasers for background illumination. Figure 3 shows a schematic diagram of the experimental arrangement.

The lasers were laboratory models (to be described separately) yielding constant intensity light-pulses of ~ 200 μsec duration for Ar II 5145 Å ($P = 30$ W) and Kr II 6471 Å ($P = 5$ W).

The discharge tube was located in one branch of the interferometer, and the probing light-beam travelled through the plasma along the tube axis. To compensate for eventual deviations due to plasma refractivity gradients, concave mirrors ($f = 300$ mm) served as optical components, and the mirror S_1 was adjusted with its center of curvature to coincide with the center of the discharge-tube axis. The resulting interference fringe patterns were separated by a prism beam-splitter (W_3) and two appropriate narrow-band transmission filters (F_1, F_2) and detected by photomultiplier tubes (VALVO 150 CVP and 150 AVP) located behind diaphragms (B_1, B_2). Sufficient stability of the total device was

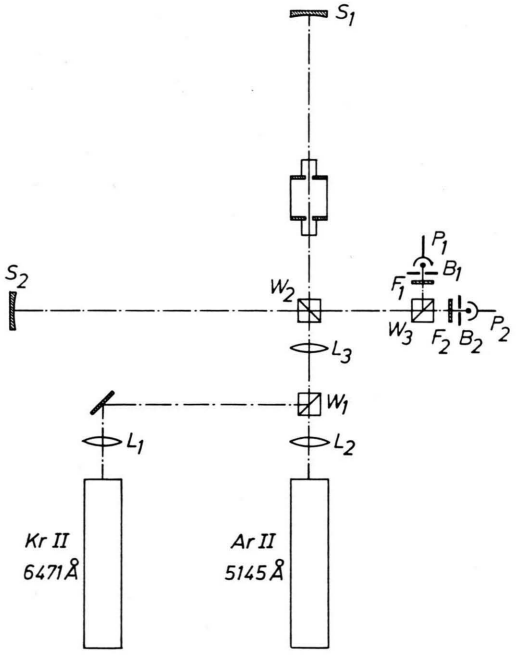

Fig. 3. Schematic diagram of the Michelson interferometer set up. L_1, L_2, L_3: lenses; W_1, W_2, W_3: beam splitters; S_1, S_2: spherical mirrors; F_1, F_2: interference filters; B_1, B_2: diaphragms; P_1, P_2: photomultipliers.

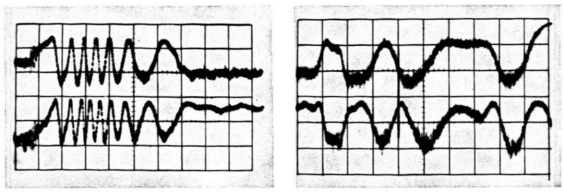

a b

Fig. 4. Typical scope traces of the interferometer output signals. Left: initial phase of the discharge 0—50 μsec. (a) Upper trace: $\lambda_1 = 5145$ Å, lower trace: $\lambda_2 = 6471$ Å. Right: time interval 45—145 μsec. (b) Upper trace: $\lambda_1 = 5145$ Å, lower trace: $\lambda_2 = 6471$ Å.

achieved by mounting all components on a framework mechanically isolated from the surroundings by pneumatic elements (tires). Changes in plasma refractivity caused the interference frings to travel across the diaphragms thus producing sinusoidal modulations of light-intensity. An example of typical scope-traces of the photomultiplier signals is given in Figs. 4; Fig. 4a shows the fringe shifts during the heating phase of the plasma, and Fig. 4b represents the quasistationary phase (upper trace: 5145 Å; lower trace: 6471 Å).

3. The Evaluation Procedure

Plasma refractivity changes and fringe shifts are related by:

$$\Delta s(\lambda) = 2/\lambda \cdot \int_0^L \Delta[n(\lambda) - 1]\,\mathrm{d}l\,, \tag{6}$$

wherein the line-integral refers to the path inside the plasma and the factor 2 accounts for the beam passing the plasma column twice. Combining (5) and (6) electron density variations are obtained from the measured fringe shifts by:

$$\int_0^L \Delta N_e\,\mathrm{d}l = -\frac{\pi m_e c^2}{e^2} \cdot \frac{0.997\,\lambda_1 \Delta s(\lambda_1) - \lambda_2 \Delta s(\lambda_2)}{0.997\,\lambda_1^2 - \lambda_2^2}\,, \tag{7}$$

wherein ΔN_e might be replaced by N_e, if the refractivity changes are determined with respect to the conditions before plasma ignition. Generally, electron density determinations from $\int N_e\,\mathrm{d}l$-values require detailed knowledge of the density profile along the line of sight. In the light-source studied here, inhomogeneous plasma layers are restricted only to the Al_2O_3-tube regions (see Figure 1). From a series of equivalent discharges (i.e. constant gas mixture, filling pressure and loading voltage), various values: $\int N_e\,\mathrm{d}l$ were determined resulting into a straight line vs. the distance between the Al_2O_3-tubes L_0. This is in agreement with the simple model of constant electron density in the path length between the tubes and inhomogeneous layers in the tubes. Electron density values were obtained from the slope: $\mathrm{d}\int N_e\,\mathrm{d}l/\mathrm{d}L_0$, covering the range $0.7-1.2 \cdot 10^{17}$ cm^{-3} with an experimental uncertainty of $\delta N_e \leqq 0.1 \cdot 10^{17}$ cm^{-3}, mainly caused by the accuracy of fringe-shift determination, whereas irreproducibilities of the light source were found to be of minor importance.

c) Plasma Temperature Determination

α) Pure Helium Plasmas

The temperatures of pure helium were derived from absolute intensity measurements of He II 3202 Å and He II 4686 Å; line profiles were obtained by the rapid-scan technique (see E, a)). The anode of a carbon-arc served — as usually — as a calibrating light source for absolute intensity determination; parameters were operated according to the specifications of Schurer [26].

In a shot-to-shot technique, the "length" of the emitting plasma column was obtained from a variation of the distance L_0 between the Al_2O_3-tubes yielding values approximately to L_0, i.e. inhomogeneous plasma layers inside the Al_2O_3-tubes might be neglected.

Temperature values were obtained from complete LTE-plasma conditions ranging from $3.6 \cdot 10^4$ to $3.9 \cdot 10^4$ K. Both lines (3202 Å and 4686 Å) yielded the same results within a $0.1 \cdot 10^4$ K-accuracy.

However, it should be mentioned, that complete LTE-conditions are not strictly valid under the plasma parameters of this experiment (see e.g. [24]), and therefore calculated temperature values might be systematically too low.

β) Helium-Hydrogen Plasmas

For line-profile determination in the He-H-plasmas, temperature values were obtained from the peak-intensity of the optically thick H_α-line, yielding approximately $1.8 \cdot 10^4$ K; more precise measurements are not necessary because line profiles are only weak functions of temperature.

F. The Results of the Present Measurements

Line profile recording and interferometric electron density determination were accomplished si-

multaneously; at least 12 line profile measurements were available for each electron density value yielding a high degree of accuracy.

From the linear variation of line-peak intensities as a function of the plasma length emission from optically thin plasma layers could be concluded.

a) The Line Profiles and the Halfwidths of the Lines He II 3203 Å *and* 4686 Å

The experimental halfwidths $\Delta\lambda_{1/2}$ of the lines He II 3203 Å and He II 4686 Å vs. electron density are shown in Figures 5. The error bars correspond to the spread of data obtained from the different series of shots; moreover, Figs. 5 present the results of previous experiments and of theoretical predictions based on the relationship:

$$\Delta\lambda_{1/2} = \left[\frac{N_e}{C(N_e, T)}\right]^{2/3}, \tag{8}$$

wherein $C(N_e, T)$ is a factor only weakly dependent on temperature and electron density, which can be taken from Griem and Shen [11], Kepple [12], and Greene [13].

Experimental results for the line He II 4686 Å are presented in Fig. 5a, agreeing well with the

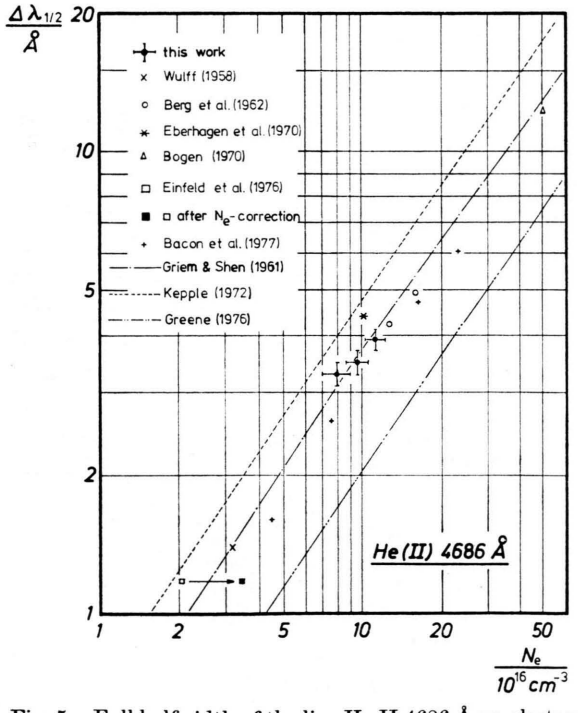

Fig. 5a. Full halfwidth of the line He II 4686 Å vs. electron density. (Theoretical curves are related to $T = 4 \cdot 10^4$ K.)

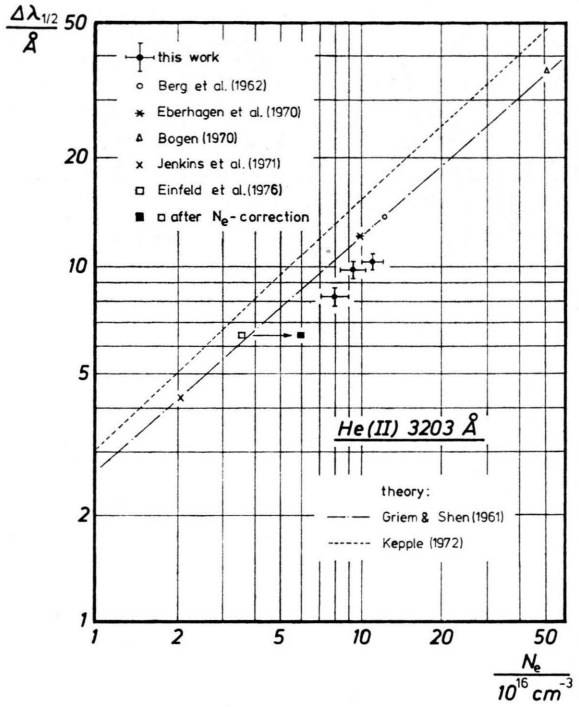

Fig. 5b. Full halfwidth of the line He II 3203 Å vs. electron density. (Theoretical curves are related to $T = 4 \cdot 10^4$ K.)

theoretical predictions of Griem and Shen [11], whereas more recent calculations of Kepple [12] and Greene [13] differ from the experimental halfwidths by more then 30%. These deviations are confirmed by measurements of Berg et al. [3], Wulff [14], and Bogen [16]. Recently published studies of Bacon et al. [18], however, yielded halfwidths for the ionic lines 15% smaller than values expected from the Griem-Shen approaches. On the contrary, Eberhagen et al. [15] and Einfeldt et al. [8] found deviations towards larger specific line widths. Referring to the latter results, electron density determination from continuous radiation was based on the line He I 5016 Å as a monitor for electron density [27], applying a correction factor 1.7 to the GBKO-calculations towards lower values. Since a number of other experiments do not confirm this contradictory result, electron densities presented in [8] might be corrected for the erroneous factor 1.7 thus yielding complete accordance with the Bacon et al. data. The halfwidths reported by Eberhagen et al. [15] were determined from θ-pinch plasma investigations ($kT = 15$—23 eV), and it seems likely that a marked influence of doubly ionized particles caused the line profile to become more broadened

than in the experiment presented here. Experimental results of Jones et al. [19] shall be compared with our results later on.

Line widths obtained from our measurements of the He II-line 3203 Å are shown in Figure 5b. Compared with the theoretical profiles of Griem and Shen [11], systematic deviations were observed towards lower line widths by $\sim 20\%$, and — with respect to the more recent calculations of Kepple [12] — the discrepancies reach 60%. This is not supported by other experiments; but it should be noted that 3203 Å-line widths of Eberhagen et al. [15] are consistent with the results of the Griem-Shen theory whereas the line width of He II 4686 Å was found to be larger by $\sim 15\%$. Assuming doubly ionized particles to influence both lines in the same way, the Eberhagen results would confirm our findings, and experimental results of Einfeldt et al. [8] provide some confirmation if corrected in the way mentioned above.

Complete line profiles of He II 3203 Å and He II 4686 Å are presented in Figs. 6; in order to enable direct comparison with theoretical results profiles are quoted in the well-known $S(\alpha)$-representation, using:

$$\alpha = \Delta\lambda/F_0 \quad \text{and} \quad S(\alpha) = (F_0/I_0)\, I(\Delta\lambda), \quad (9)$$

wherein: $\Delta\lambda = \lambda - \lambda_0$ is the distance from the line-center in Å-units; $F_0 = 2.606\, e N_e^{2/3}$ is the normal fieldstrength in cgs-units, and $I_0 = \int I(\Delta\lambda)\, \mathrm{d}\lambda$ is the total line intensity.

In the expression for F_0 corrections for doubly ionized particles were neglected, and experimental total line intensities I_0 were evaluated applying the asymptotic formula $\sim \Delta\lambda^{-5/2}$. Error bars attributed to the line wings correspond mostly to uncertainties in the subtraction of the underlying continuum.

Figure 6 a shows the experimental profiles of the line He II 4686 Å together with theoretical results of Griem and Shen [11], Kepple [12], and Greene [13]. Comparing the results from the measurements with the calculations [11] and [12], experimental line shapes exhibit increased line peaks but lower line wings. On the contrary, approaches of Greene [13] yield a rather narrow line center, whereas the line wings are in fairly good agreement with our measurements.

Experimental $S(\alpha)$-profiles obtained from preceding investigations ([14], [15], [16], and [19]) are presented in Fig. 6a, too. Line wing intensities from [14] and [16] approach the results of this work

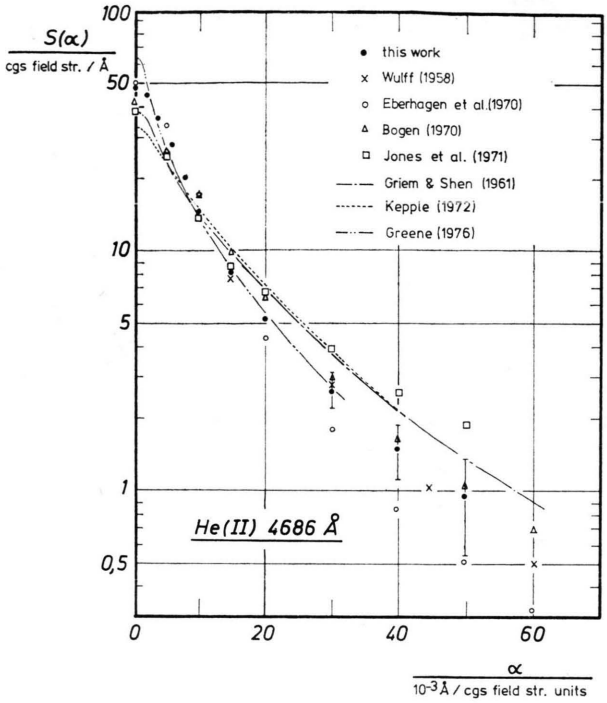

Fig. 6a. Area-normalized profiles of the line He II 4686 Å. The theoretical profiles are related to $N_e = 10^{17}$ cm^{-3} and $T = 4 \cdot 10^4$ K. The experimental values of Jones et al. [19] (□) are corrected for the erroneous α-scale (× 10)*.

rather well; peak intensities reported in [16] are somewhat lower due to the slightly broader $S(\alpha)$-profiles [11] caused by the higher electron density conditions there. Line profiles presented in [15] account for the influence of doubly charged perturbing particles applying a proper correction to the normal fieldstrength; but in spite of this modification wing intensities are significantly lower than found in this work. Finally it should be noted, that far line wing intensities of [19] exceed — in contrast to all other experiments — the theoretically predicted values, probably caused by inhomogeneities of the plasma source or by underlying oxygen lines. α-values in [19] are erroneous and by a factor of 10 too low*; for comparison in Fig. 6a correction has been made.

In Fig. 6b experimental profiles of the line He II 3203 Å are compared with theoretical results [11], [12]. Discrepancies between both line shapes are similar to those obtained for the 4686 Å-line, but the central dip proved to be deeper than predicted by the Griem-Shen theory. In addition, Fig. 6b

* Private communication: H. R. Griem.

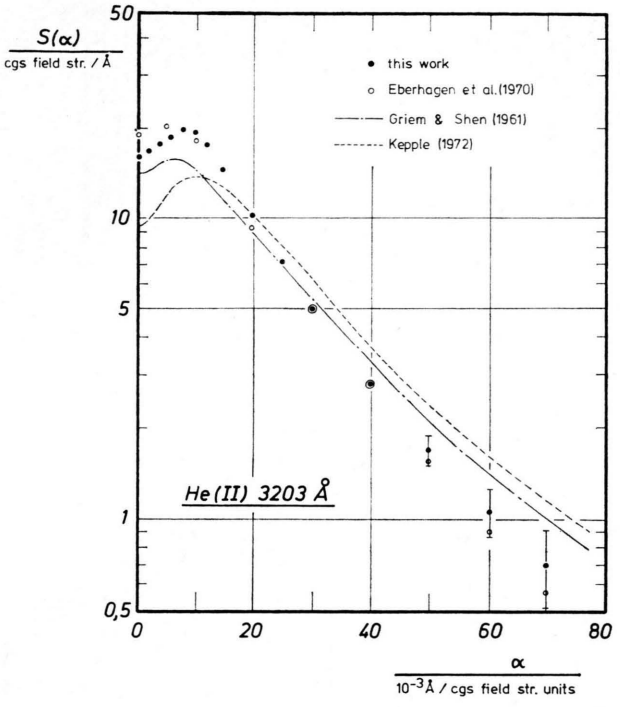

Fig. 6b. Area-normalized profiles of the line He II 3203 Å. The theoretical profiles are related to $N_e = 10^{17}$ cm^{-3} and $T = 4 \cdot 10^4$ K.

presents an experimental profile of Eberhagen et al. [15], also showing lower intensities in the far line wings.

b) The Line Profiles and the Halfwidths of the Lines He I 3188 Å, 3889 Å, *and* 5016 Å

Experimental studies on neutral helium line profiles were performed on mixed He-H plasmas; pure helium plasmas were not suitable here because of the important role of He I-emission from inhomogeneous plasma layers, due to the maximum of line emission at norm-temperatures $\sim 2.4 \cdot 10^4$K, whereas homogeneous regions of the plasma had temperature values near to $4 \cdot 10^4$ K. In mixed He-H plasmas, however, temperature values of the homogeneous bulk plasma were reduced below the norm-temperature causing He I-emission mainly from this part of the plasma column. Remaining influence of inhomogeneous layers could be restricted by evaluating line profiles only from shots at large plasma lengths (the distances of the inner ends of the Al_2O_3-tubes $\geqq 7$ cm). Significant line-reversal was only observed at the intense line He I 5876 Å, which therefore was not further investigated.

Emission from optically thin layers was proved by comparison of the line-peak intensities with the black-body radiation function, yielding always optical depth values $\leqq 0.05$.

Figures 7a—c present experimental halfwidths of the lines He I 3188 Å, 3889 Å, and 5016 Å compared with theoretical results from the GBKO-approach [2], yielding (full) halfwidths related to electron density values by the approximation formula:

$$\Delta\lambda_{1/2} = 2w[1 + 1.75\alpha(1 - 0.75r)] \cdot 10^{-16} N_e; \quad (10)$$

herein $2w$ is the (total) width due to electron impacts; α denotes the ion-broadening parameter, and r is the ratio: mean distance between ions/Debye-radius; theoretical values for w and α are published by Griem [1].

As can be seen from the figures, predictions from GBKO-theory are confirmed by this experiment within $\pm 10\%$, and this result is in accordance with most other experiments performed so far.

Neutral helium halfwidths reported by Greig et al. [5] differred by $\sim 15\%$ from GBKO-theoretical results; re-examination in a later work [6] achieved agreement with theory, as well as Berg et al. [3], within the experimental accuracy. Discrepancies by a factor 1.7 — as determined by Kusch [7] for the lines He I 3889 Å and 5016 Å, and by Einfeldt et al. [8] for the line He I 5016 Å — were evidently caused by plasma column inhomogeneities.

In the first case [7], helium line profiles calibrated by H_β-electron densities were obtained by end-on observation through slots in the electrodes, favoring plasma emission from regions of different temperature (which is severe accounting for the different norm-temperature values: He I: $2.4 \cdot 10^4$ K and H_β: $1.6 \cdot 10^4$ K) thus causing H_β-emission mainly from the lower temperature parts along the line of sight and leading to the observed discrepancy.

In the second case [8], electron density values were determined from continuous radiation related to a scale obtained via the He I-line 5016 Å applying Stark broadening parameters from an earlier experiment [27], which sufferred from inhomogeneous plasma emission too.

Finally, in Fig. 8 experimental line profiles of He I 5016 Å are shown in comparison with theo-

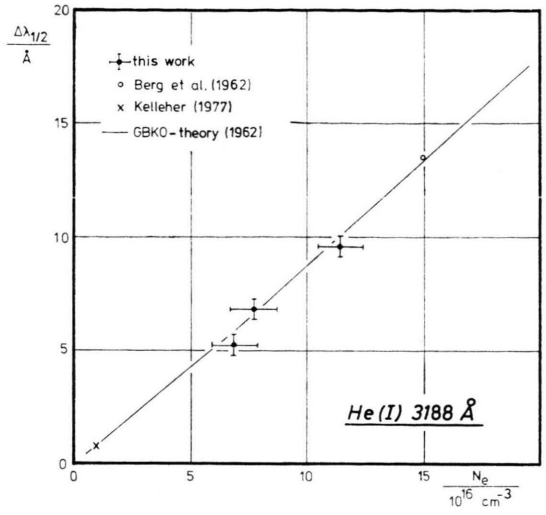

a

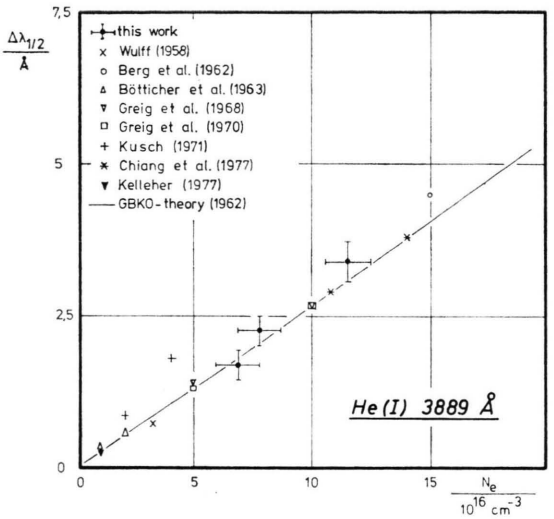

b

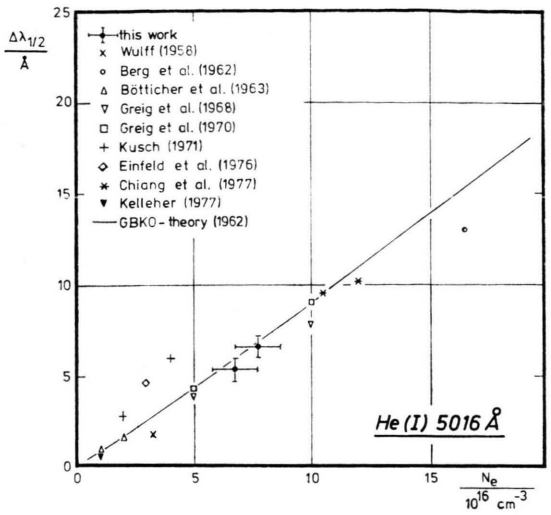

c

Figs. 7a–c. Full halfwidths of neutral helium lines vs. electron density. Theoretical curves are related to $T = 2 \cdot 10^4$ K.

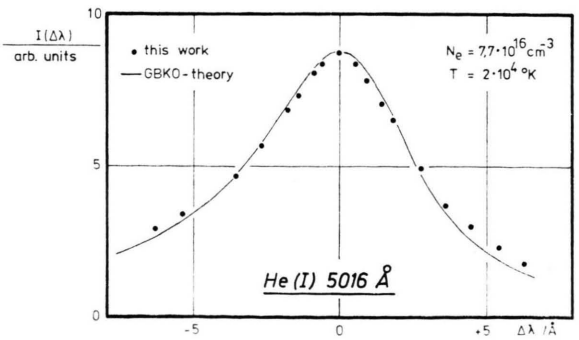

Fig. 8. Experimental and theoretical profile of the line He I 5016 Å normalized to equal peak intensity.

retical line shapes from the GBKO-theory; both profiles are normalized to equal peak intensity for better presentation. Apart from minor discrepancies — probably caused by the far wings of neighboring lines — profiles agree well, and the measured asymmetry corresponds to the theoretical predictions indicating plasma inhomogenities to be of no importance in this experiment.

Acknowledgements

The authors are greatly indebted to the Deutsche Forschungsgemeinschaft for personal and equip-

ment support. Fruitful discussions with Dr. H. Ehrich, Dr. G. Röndigs, and B. Huhn were helpful in all phases of the work, which one of us (H.S.) has submitted to the Science Department of Kiel University in partial fulfillment of the requirements of his thesis.

[1] H. R. Griem, Spectral Line Broadening by Plasmas. Academic Press, New York 1974.
[2] H. R. Griem, M. Baranger, A. C. Kolb, and G. Oertel, Phys. Rev. **125**, 177 (1962).
[3] H. F. Berg, A. W. Ali, R. Lincke, and H. R. Griem, Phys. Rev. **125**, 199 (1962).
[4] W. Bötticher, O. Roder, and K. H. Wobig, Z. Physik **175**, 480 (1963).
[5] J. R. Greig, C. P. Lim, G. A. Moo-Young, G. Palumbo, and H. R. Griem, Phys. Rev. **172**, 148 (1968).
[6] J. R. Greig and L. A. Jones, Phys. Rev. A **1**, 1261 (1970).
[7] H. J. Kusch, Z. Naturforsch. **26a**, 1970 (1971).
[8] D. Einfeldt and G. Sauerbrey, Z. Naturforsch. **31a**, 310 (1976).
[9] W. T. Chiang, D. P. Murphy, Y. G. Shen, and H. R. Griem, Z. Naturfosch. **32a**, 818 (1977).
[10] D. E. Kelleher, Techn. Note BN-865, Univ. of Maryland (1977).
[11] H. R. Griem and K. Y. Shen, Phys. Rev. **122**, 1490 (1961).
[12] P. C. Kepple, Phys. Rev. A **6**, 1 (1972).
[13] R. L. Greene, Phys. Rev. A **14**, 1447 (1976).
[14] H. Wulff, Z. Physik **150**, 614 (1958).
[15] A. Eberhagen and R. Wunderlich, Z. Physik **232**, 1 (1970).
[16] P. Bogen, Z. Naturforsch. **25a**, 1151 (1970).
[17] J. E. Jenkins and D. D. Burgess, J. Physics B **4**, 1353 (1971).
[18] M. E. Bacon, A. J. Barnard, and F. L. Curzon, J. Quant. Spectr. Rad. Transfer **18**, 399 (1977).
[19] L. A. Jones, J. R. Greig, T. Oda, and H. R. Griem, Phys. Rev. A **4**, 833 (1971).
[20] R. A. Alpher and D. R. White, Optical Interferometry, in: Plasma Diagnostic Techniques, Eds. R. H. Huddlestone and S. L. Leonard, Academic Press, New York 1965.
[21] H. J. Kusch and E. R. Mewes, Z. Naturforsch. **22a**, 676 (1967).
[22] A. D. Stokes, J. Opt. Soc. Amer. **57**, 1100 (1967).
[23] R. Rompe and H. Steenbeck, Progress in Plasmas and Gas Electronics, Vol. I, Akademie-Verlag, Berlin 1975.
[24] H. R. Griem, Plasma Spectroscopy, McGraw-Hill, New York 1964.
[25] C. W. Allen, Astrophysical Quantities, Athlone Press, London 1955.
[26] K. Schurer, Appl. Optics **7**, 461 (1968).
[27] D. Einfeldt and G. Sauerbrey, Z. Naturforsch. **30a**, 1413 (1975).